

Multi-Scale Modeling of Processing of Carbon Nanotubes

Hyuk Soon Choi, Kwang Hee Kim, Ki-Ha Hong, Jongseob Kim, Hyo Sug Lee and Jai Kwang Shin
Samsung Advanced Institute of Technology, San 14-1 Nongseo-Ri, Giheung-Eup, Yongin-Si
Gyeonggi-Do, Republic of Korea 449-772

A. V. Vasenkov, A. I. Fedoseyev, and Vladimir Kolobov
CFD Research Corporation, 215 Wynn Drive, Huntsville, AL 35805
Gyeonggi-Do, Republic of Korea 449-772

ABSTRACT

As technologies are continuously advancing, new semiconductor materials and novel devices are being developed which are indispensable for electronic applications. Progress in the computer aided design of fabrication of nanoscale materials lags behind experimental advances, since atomistic simulation methods are computationally impractical, while mesoscopic simulation methods are not capable of capturing nanoscale effects. Multi-Scale Computational Framework is introduced to conduct over 3 scales, continuum model of reactor-scale processes, kinetic Monte Carlo for the growth of nanostructures, and molecular dynamics for the prediction of reaction rates. "Gap-tooth" algorithm and "coarse time-stepper" method are employed to couple the scales. The results of multiscale simulation for growth of carbon nanotubes by plasma enhanced chemical vapor deposition are presented.

Keywords: Multiscale Simulation, Coarse Time-Stepper, Gap-Tooth, Plasma Enhanced Chemical Vapor Deposition (PECVD), Carbon Nanotube (CNT).

1 DESCRIPTION OF THE FRAMEWORK

The rapid development of nanotechnology has created significant interest to predicting the behavior of materials from the atomic to the engineering scales. For simulation of processes over the length and time scales that are a million times disparate, Multi-Scale Computational Framework (MSCF) has been developed by coupling computational tools of different types. The computational fluid dynamics (CFD) simulation was employed in reactor-scale, while atomistic kinetic Monte Carlo (kMC) and molecular dynamic (MD) simulations were performed in microscopic region to describe behaviors of atoms and molecules. The feasibility of the developed framework was shown using reactor-scale CFD-ACE software with plasma simulation capabilities [1], NAMD code designed for molecular systems [2], and kMC-FILM software developed for the deposition of nanostructured films and growth of carbon nanotubes.

The interactions between different kMC modules can be outlined as follows. The Interface control module receives initial data, transfers these data to other modules and also calls other modules to perform simulations of different processes. The Transport module calculates the transport of gas species from the source plane to the surface. The surface kinetic module calculates surface reactions between gas and surface species and computes surface fluxes and fluxes of carbon absorbed on the surface of catalyst. The surface fluxes are used by the FILM/CNT growth module and the carbon fluxes are sent to the Catalytic Interface module. The Catalytic Interface module calls continuum solver to simulate the diffusion of absorbed carbon through the catalyst and compute fluxes of carbon atoms to be incorporated into CNTs. The CNT/FILM module simulates the growth of CNT on the surface of catalyst and the formation of crystal film on other surfaces. The Output module writes the growth and visualization data to output files.

The Gap-tooth module was used to couple kMC simulations in teeth with CFD simulations in large gaps particularly, incoming microscopic surface fluxes and number of particles to a tooth at each tooth boundary were updated using the microscopic surface fluxes and number of particles outgoing from the nearest.

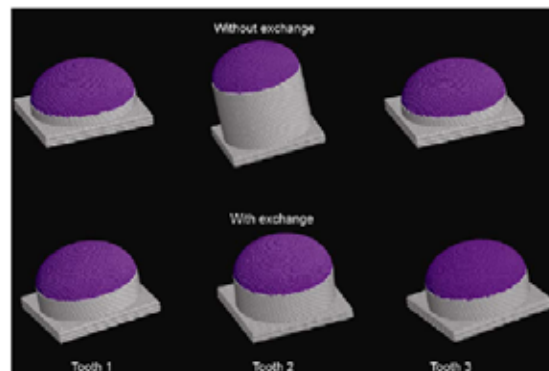


Figure 1: Growth of carbon nanotubes with (top) and without (bottom) gap-tooth method for teeth of low and high reactant fluxes from reactor.

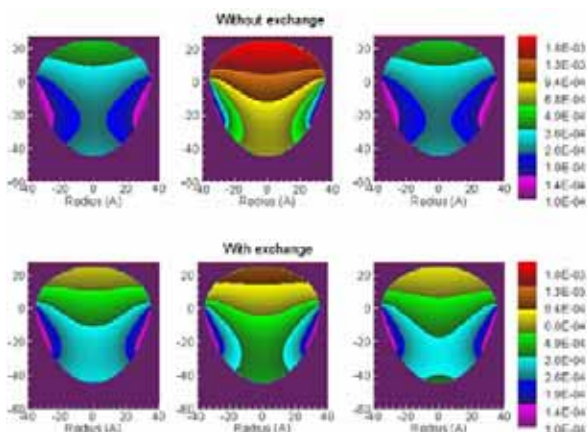


Figure 2: Carbon concentration profiles in the catalyst of teeth of low and high reactant fluxes from reactor with (top) and without (bottom) gap-tooth method .

To verify effect of gap-tooth method, the growth and carbon concentration profile were calculated for the carbon nanotubes with low and high reactant fluxes from reactor scale. Tooth 1 and 3 have low C_2H_2 flux of $1.0 \cdot 10^{16} / \text{cm}^3$ and tooth 2 has high C_2H_2 flux of $2.0 \cdot 10^{17} / \text{cm}^3$, 20 times larger than tooth 1 and 3, while other reactant species fluxes are kept identical. Fig. 1 and Fig. 2 show the effect of gap-tooth method to distribute the reactant hydrocarbon flux to nearest teeth, i.e. carbon nanotubes, by allowing the transport the reactants between teeth. Resultantly, the growth rate of carbon nanotube with high flux decreases and those of carbon nanotube with low flux increases by getting reactant species from high flux neighbor.

Two choices of flux interpolation were implemented in the Gap-tooth module: linear flux interpolation and quadratic flux interpolation. In both cases, incoming microscopic surface fluxes and number of particles to a tooth were computed using the microscopic surface fluxes and number of particles outgoing from the nearest teeth as described in earlier report [3].

The coarse timestepper module was developed to bridge the differences in the time scales between kMC and MD. The major steps of the Coarse Timestepper module are:

- Set initial configurations for NAMD simulations by cloning MD spatial coordinates from those of corresponding kMC simulations.
- Perform the evolutions of molecular systems. The evolutions were performed for the time T_{MD} long enough compared to MD time step τ_{MD} of 10 femto seconds and short enough compared to kMC time step τ_{KMC} of a few microseconds. Each NAMD ensemble was at fixed volume, temperature, and the number of particles.

- Calculate rates, and their derivatives in respect to time. Accuracy required for the prediction of reaction rates was achieved due to the use of reactive MD approach. This approach employs pre-defined criteria in bond-breaking/bond-making routine and it has been successfully used for computing rates of thermal decomposition reactions in polymers [4].
- Project reaction rates to the time $t + \tau_p$ such that $T_{MD} \leq \tau_p \leq \tau_{KMC}$. The projection is achieved using the Newton-Raphson method.

The interactions between different modules of MSCF over a mesoscopic time step τ are conducted as follows. MD was performed in each tiny tooth to compute the rates of surface processes and their derivatives in time for a nanoscopic time. The MD results were transferred to the Coarse timestepper module which calculated the time-dependent rates using the Newton-Raphson method. The rates were used by kMC to model system evolution during a microscopic time step. Subsequent to each kMC iteration, the incoming fluxes for each tooth were updated by the Gap-tooth module from the fractions of outgoing kMC fluxes obtained in the nearest teeth and MD was called by the Coarse timestepper module for updating time-dependent rates. Once the simulation time in kMC reaches $t + \tau$, the CFD solver was called by the Gap-tooth module to simulate reactor-scale processes and compute the fluxes of absorbed species for kMC.

2 GROWTH SIMULATIONS OF CARBON NANOTUBES BY PLASMA ENHANCED CHEMICAL VAPOR DEPOSITION (PECVD)

MSCF was applied to simulate the plasma assisted growth of aligned CNTs in an Inductively Coupled Plasma (ICP) reactor in a CH_4/H_2 gas mixture in Fig. 3. In this reactor, plasma is sustained by radio frequency (RF) electro-magnetic fields created by an RF current in a coil [2].

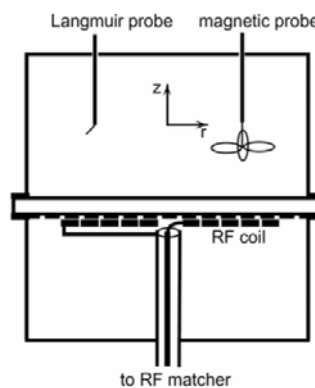


Figure 3: The schematic of ICP reactor.[5]

The calculated electron concentration, gas temperature and concentrations of C_2H_2 and CH_3 species are shown in Fig. 4 for a gas pressure of 100 mTorr, 100 W power adsorbed in plasma, and a driving frequency of 6 MHz. The substrate temperature was kept at 1000 K. The electron density peaks in the center of the reactor, the gas temperature has two peaks: one near the substrate and the other near the coils. The C_2H_2 and CH_3 densities peak near the sidewall where the gas temperature is low.

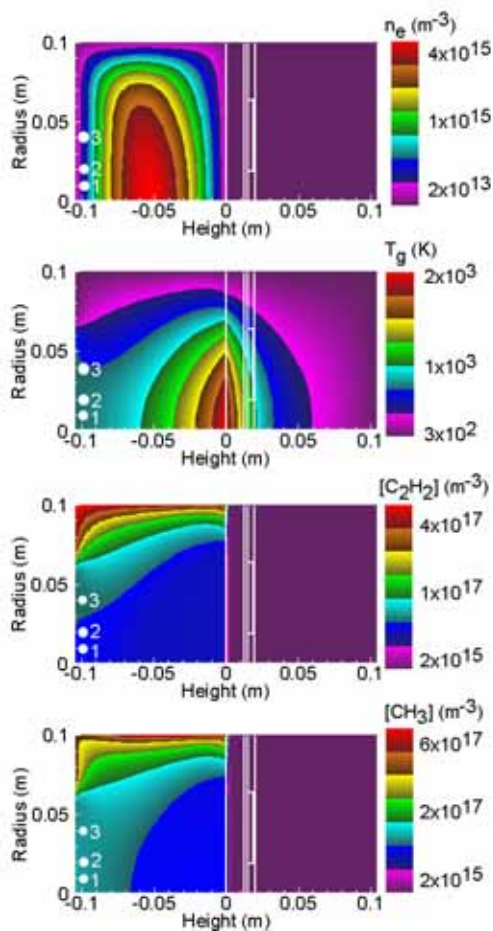


Figure 4: Plasma and gas properties computed by CFD-ACE for ICP plasma sustained in CH_4/H_2 . White spots represent locations of monitor points where fluxes of radicals were transferred from CFD to kMC solvers.

The fluxes of different radicals computed by CFD-ACE at selected monitor points were used to update on-the-fly kMC-FILM fluxes. The growths of CNTs of different diameters were calculated using these fluxes as shown in Fig. 5. For example, CFD-ACE fluxes at the 1st monitor point were used for the growth of two CNT of small

diameter (35 \AA). At the same time, CFD-ACE fluxes at the 2nd monitor point were used for the growth of two CNT of small diameter (35 \AA) and one CNT of large diameter (58 \AA). Finally, CFD-ACE fluxes at the 3d monitor point were used for the growth of two CNT of large diameter (58 \AA).

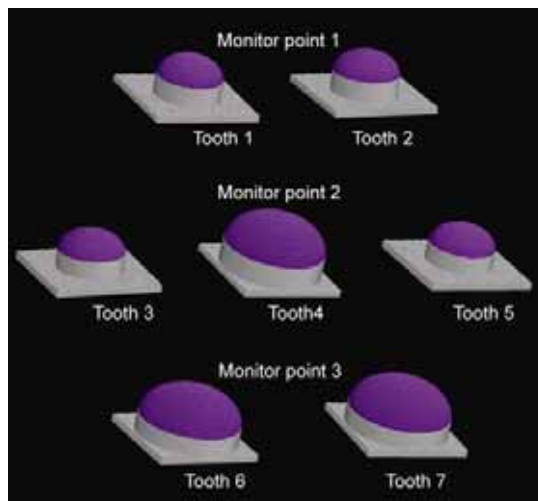


Figure 5: The growth of CNTs on the catalyst of different size at chosen monitor points.

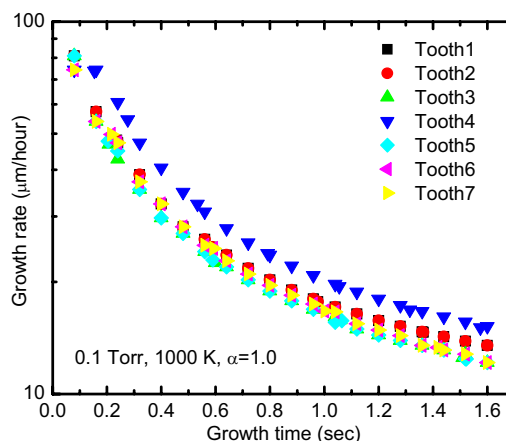


Figure 6: The growth rates. The largest growth rate is in the 4th tooth due to data exchange between 3rd, 4th and 5th teeth. The growth rates in 1st and 2nd teeth are slightly higher than those in the 6th and 7th teeth.

The growth rates of CNTs in seven teeth are shown in Fig. 6. It was observed that the growth rates of CNTs in the 1st and 2nd teeth with small catalyst are larger than those in

the 6th and 7th teeth with large catalyst. In contrast, the growth rate in the 4th tooth with large catalyst is larger than that in the 3rd and 5th teeth with small catalyst. The reason for the described trends is as follows. The light hydrocarbon specie can react on both catalyst surface and substrate surface, while heavy hydrocarbon radicals dominantly react on the surface of catalyst. Consequently, in the teeth with small catalyst, the ratio of heavy species to light species increases with time since heavy species react only on a portion of the tooth's surface. As the fraction of heavy species increases, the growth rates of CNT in 1st and 2nd teeth also increase compared to those in the 6th and 7th teeth. This is due to the thermal decomposition of heavy hydrocarbon radicals on the surface of catalyst. At the same time, data exchange between 3rd, 4th, and 5th teeth increases the ratio of heavy species to light species in the central tooth and decreases this ratio in the side teeth.

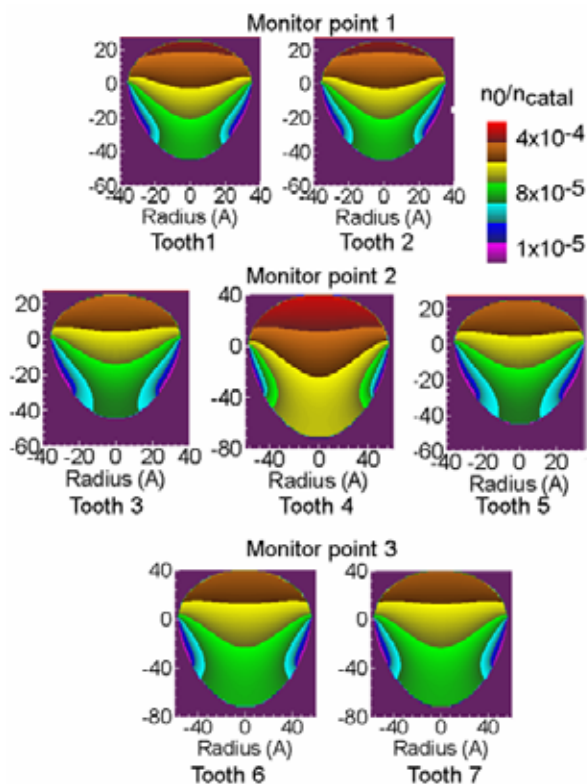


Figure 6: The concentrations of carbon inside of catalysts of different size.

The concentration of carbon inside catalytic particle is shown in Fig. 6. Similar to the growth rate, the peak concentration is achieved inside the catalytic particle located in the 4th tooth. The peak concentration in this tooth is about two times larger than that in the 3rd and 5th teeth.

This is due to the increase of the ratio of heavy hydrocarbon to light hydrocarbons in the 4th tooth and decrease of this ratio in the 3rd and 5th teeth as a result of boundary data exchange. The concentrations of carbon in the 1st and 2nd teeth are 30% larger than those in the 6th and 7th teeth as a result of differences in both catalyst size and input fluxes computed by CFD-ACE.

3 CONCLUSIONS

The multi-scale computational framework (MSCF) which couples continuum model, kMC simulation, and molecular dynamics method has been developed for nanostructured materials' fabrication. The validation was performed for the plasma-assisted growth of vertically aligned CNTs in a realistic CH₄/H₂ ICP system. It was found that boundary data exchange between regions where atoms self-assemble into CNTs of different size substantially affected the simulation results.

REFERENCES

- [1] V. I. Kolobov, *Comput. Materials Sci.* **28**, 302, 2003
- [2] L. Kale, R. Skeel, N. Bhandarkar, R. Brunner, A. Gursoy, N. Krawetz, J. Phillips, J. Shinozaki, K. Varadarajan, and K. Schulten, *J. Comput. Physics* **151**, 283, 1999.
- [3] C. W. Gear, J. Li, and I. G. Kevrekidis, *Phys. Lett. A* **316**, 190, 2003.
- [4] S. I. Stoliarov, P. R. Westmoreland, M. R. Nyden, and G. P. Forneyb, *Polymer* **44**, 883, 2003.
- [5] Godyak, V. A., R. B. Piejak, *Plasma Sources Science and Technology* **11**(4): 525-543, 2002.